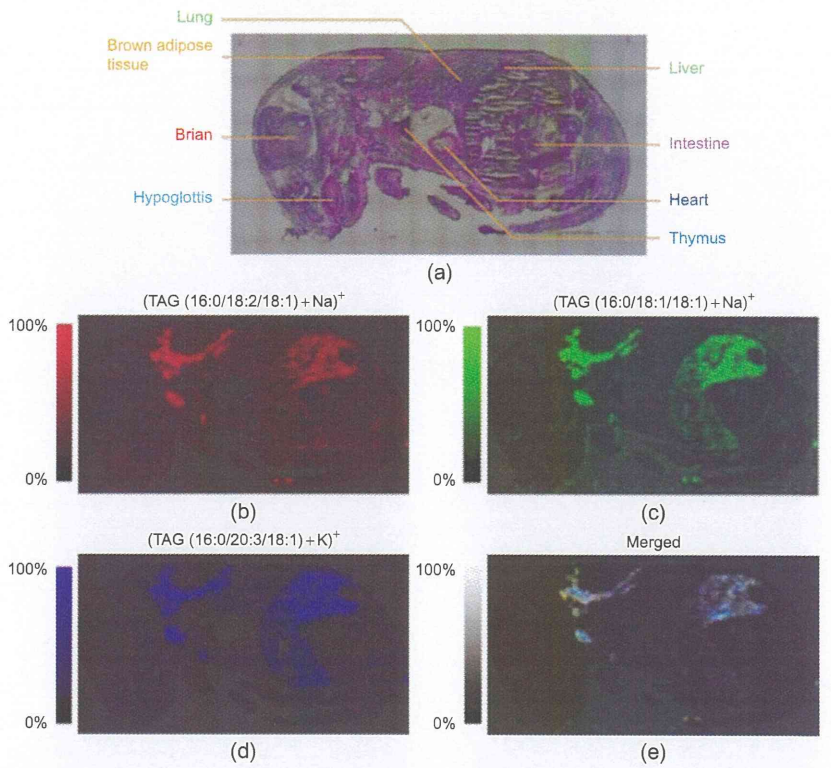

FIGURE 16 MALDI-IMS of neutral lipids. Distribution of triglycerides (TAG) in mouse embryo. (a) H&E staining, (b) ion images of $[TAG\ (16{:}0/18{:}2/18{:}1)+Na]^+$, $[TAG\ 16{:}0/18{:}1/18{:}1)+Na]^+$, and $[TAG\ (16{:}0/20{:}3/18{:}1)+K]^+$ are shown. (b)–(d) The ion images were merged with the optical image of an H&E-stained section. (e) Three merged TAG images demonstrate the same distribution. Reprinted from Hayasaka *et al.* (2009) with permission from Springer.

7.2. IMS for Proteomics

The study of proteomics is useful for biomarker discovery of a large number of diseases, using tissue samples such as vascular tissue, heart, brain, lung or bone, with a current major focus on cancer and malignant tissues (MacAleese *et al.*, 2009). Today MALDI-IMS is increasingly being used for direct analysis of peptides and proteins from tissue sections; the main advantage is that it requires no labeling reagents (McDonnell and Heeren, 2007; Stoeckli *et al.*, 2001). Immunohistochemistry (IHC) has long been the standard technology for imaging of peptide and protein distribution in tissue. The sensitivity of IHC is usually excellent. However, this method requires a specific binder, usually an antibody, to detect a previously defined protein from the sample. Only a very small number of molecules may be detected in parallel, and these all need to be known beforehand.

Antibody availability and specificity are other constraints with IHC that limit its capacity (Luongo de Matos *et al.*, 2010). Thus the introduction of IMS has provided complementary resources.

What IMS lacks in terms of sensitivity, it compensates for by enabling untargeted studies with the possibility to detect hundreds of molecules in a single run. In the so-called bottom-up approach, the proteins present in the tissue sample must first be subjected to *in situ* digestion by a proteolytic enzyme. Usually trypsin is used since it renders peptides that contain at least one lysine or arginine amino acid and hence are easily ionized. Setou *et al.* (2008) investigated whether the addition of detergent into the trypsin solution could improve the digestion efficiency of proteins for direct analysis of tissue section in MALDI-.IMS. Trypsin solution can be spotted directly onto the tissue sections, rendering spot sizes ~150–200 μm. Considering the possibility for peptide migration within this spot area, the tryptic spot size can also be said to determine the resolution of the IMS experiment, although the spatial resolution from the actual data acquisition is determined by the instrument used and is usually lower. Organic matrices such as DHB and CHCA are used for ionization.

For biomarker studies, the tissues available through biobanks around the world have generally been treated with formalin for increased tissue stability over time. Formalin fixation and subsequent paraffin embedding allows for stable histomorphology, but it also causes difficulty in IMS since it cross-links proteins and hampers protein mining. This problem has been overcome by deparaffinization methods followed by the same antigen-retrieval methods used in IHC experiments (enzymatic or heat-mediated) (Aoki *et al.*, 2007). Recently formalin-fixed, paraffin-embedded tissue microarrays were analyzed in MALDI-IMS and MS/MS experiments to study the gastric carcinoma tissue, thereby identifying the histone (H4)-specific signal in poorly differentiated cancer tissue samples (Morita *et al.*, 2010). Other groups have demonstrated the direct analysis and identification of tryptically digested proteins from tissue samples of lung cancer (Groseclose *et al.*, 2008), breast cancer (Ronci *et al.*, 2008), prostate cancer (Cazares *et al.*, 2009), and pancreatic adenocarcinoma (Djidja *et al.*, 2009). Chaurand *et al.* (2004) showed the level of the binding protein (S100B) in tissue samples using MALDI imaging to distinguish a high-grade and low-grade glioma. In addition, the combined approach of MALDI-IMS and MS/MS analyses of digested myelin basic protein (MBP) in a coronal section of rat brain has been demonstrated (Figure 17a–c) (Groseclose *et al.*, 2007). After digestion, a total of eight tryptic peptides from MBP were detected (Figure 17d). This protein is essential for the formation of myelin in the central nervous system. MALDI-IMS also has been used to classify a pancreatic cancer tissue microarray where a number of proteins that appear to discriminate between different tumor classes were detected (Djidja *et al.*, 2009). Direct proteomic-based imaging was also performed

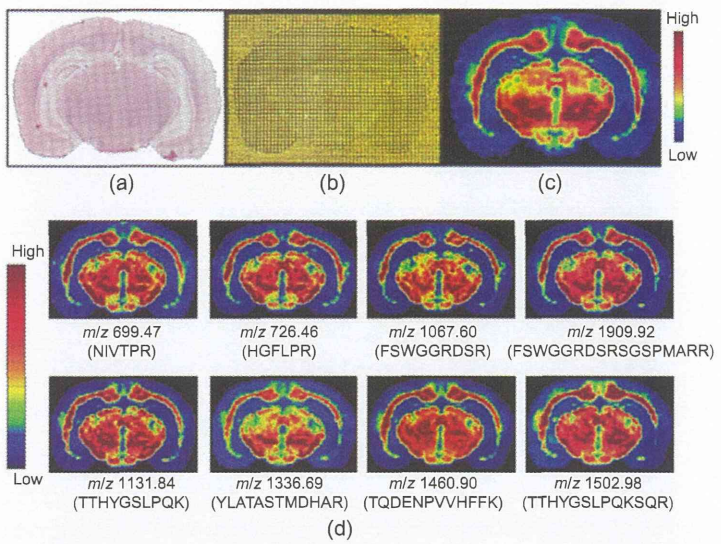

FIGURE 17 (a) H&E stain of rat brain tissue section serial to the sections used for digestion and imaging. (b) Tissue section spotted with a sinapinic acid matrix solution. (c) Image of the 14.2-kDa isoform of myelin basic protein. (d) Images of 8-tryptic peptides generated from the digestion of the 14.2-kDa isoform of myelin basic protein. Reprinted from Groseclose *et al.* (2007) with permission from John Wiley and Sons.

on a gene knockout mice tissue section of rat that could be useful for the diagnosis of human diseases (Yao *et al.*, 2008). Figure 18 shows the PCA of mass spectra from Scrapper-knockout (SCR-KO) and WT mouse brains analyzed by MALDI-IMS.

7.3. IMS for Pharmacokinetic Studies

Imaging of pharmaceuticals samples is performed to examine pharmacokinetics—that is, the absorption, distribution, metabolism, and excretion of drugs in laboratory animals and humans. HPLC combined with MS/MS is used to analyze and characterizze most drugs. However, HPLC-MS/MS analyses cannot provide the distribution of drugs in different organs or tissues of laboratory animal experiments (Hsieh *et al.*, 2003). Whole-body autoradiography (WBA) is normally used for the visualization of drug candidates in all tissues; however, it requires the compound of interest to be radioactively labeled (Kertesz *et al.*, 2008). This disadvantage of WBA can be overcome by using MALDI-IMS to analyze the drugs in tissue samples. The drug distribution profile obtained by IMS tells whether the oral administration of an exogenous compound affects the endogenous metabolites (Rubakhin *et al.*, 2005). Reyzer *et al.* (2003) reported images of two antitumor drugs in mouse tissue samples using

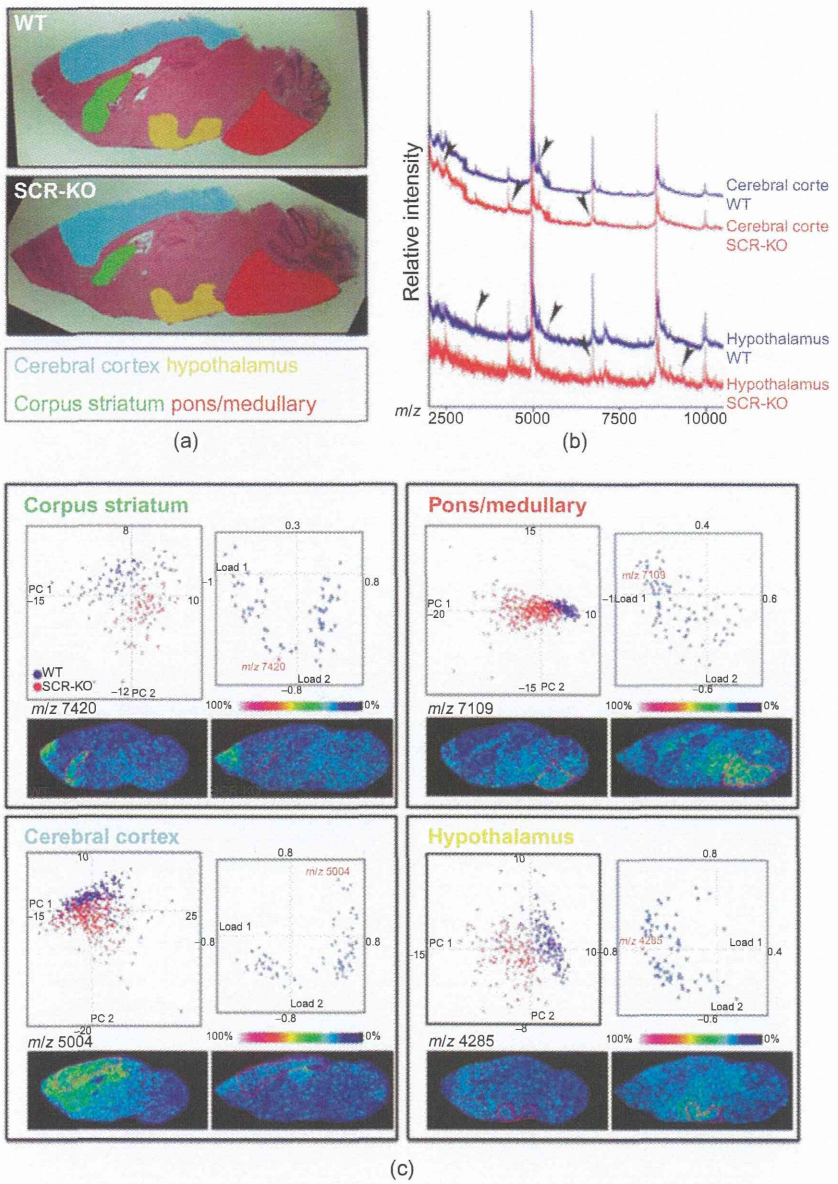

FIGURE 18 *In situ* proteomics of the SCR-KO mouse brain using IMS and PCA. (a) H&E-stained images of the WT and SCR-KO mouse brain. The regions focused in IMS analyses are indicated by colors. (b) Mass spectra obtained from each region of the WT or SCR-KO mouse brain sections. Specific signals of the regions are indicated by arrowheads. (c) Distributions of principal component scores of mass spectra from various brain regions (left spray graphs; WT, blue; KO, red) and the loading factors plot (right graphs). The signal intensities of mass spectra of the substances with indicated m/z are shown in the reconstructed images of the mouse brain analyzed by IMS. Reprinted from Yao *et al.* (2008) with permission from John Wiley and Sons.

MALDI-IMS. The results showed the spatial distributions of drugs in brain tissue section were elucidated using a Q-TOF instrument operated in selective reaction monitoring (SRM) mode to provide good sensitivity for tissue analysis. This work demonstrated the proof of MALDI-IMS in monitoring a drug distribution in different parts of body organs. MALDI-IMS can provide the spatial information for both drugs and their metabolites. Figure 19a–d shows the distributions of the drug olanzapine and its metabolites (*N*-desmethyl metabolite and 2-hydroxymethyl) in tissue after post dosing of 2 hours and 6 hours (Khatib-Shahidi *et al.*, 2006). Further,

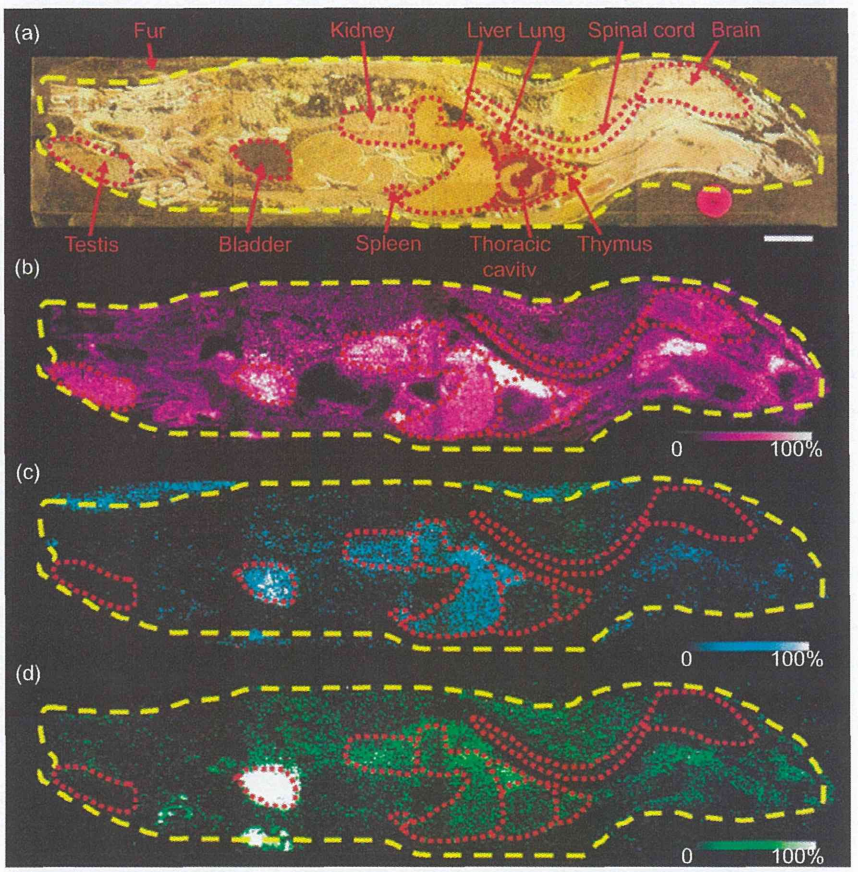

FIGURE 19 Detection of drug and metabolite distribution at 2 hours after dosing in a whole rat sagittal tissue section using IMS analysis. (a) Optical image of a 2-hr post olanzapine-dosed rat tissue section across four gold MALDI target plates Organs are outlined in red. A pink dot used as a time point label. (b) MS/MS ion image of olanzapine (m/z 256). (c) MS/MS ion image of *N*-desmethyl metabolite (m/z 256). (d) MS/MS ion image of 2-hydroxymethyl metabolite (m/z 272). Scale bar, 1 cm. Reprinted from Khatib-Shahidi *et al.* (2006) with permission from American Chemical Society.

SIMS and NIMS were used for imaging of drugs in tissue samples and the mass spectrum obtained was free of the matrix-oriented peaks. The direct analysis of clozapine and its metabolites in dosed rat brains has been illustrated using TOF/TOF mass analyzers (Yanes *et al.*, 2009). NIMS-IMS is compatible with both ion beam and laser sources available on commercial SIMS and MALDI instruments. In addition, fewer laser shots are required per spot compared with the MALDI technique.

7.4. IMS for Metabolomics

Metabolomics is the study of metabolites, including metabolic intermediates such as lipids, amino acids, organic acids, and small signaling molecules. Concentration changes of metabolites in tissue samples might reflect a specific physiological or pathological condition of the organism (Dunn, 2008; Nicholson and Lindon, 2008). Liquid chromatography–mass spectrometry and gas chromatography–mass spectrometry are well-known techniques for metabolite analysis (Griffiths and Wang, 2009; Novotny *et al.*, 2008). Here, the tissue samples are homogenized before analysis and thus it is impossible to assess their actual tissue distribution. However, IMS can be directly used to profile a broad range of small molecules, including nucleotides, amino acids, proteins, lipids, and carboxylic acids, in tissue samples with their unique distributions. MALDI-IMS has been used for imaging and identification of 13 primary metabolites, such as adenosine monophosphate (AMP), adenosine diphosphate (ADP), adenosine triphosphate (ATP), uridine diphosphate (UDP), or *N*-acetyl-D-glucosamine (GlcNAc) in rat brain sections (Benabdellah *et al.*, 2009). The distribution pattern of lipids such as cholesterol, cholesterol sulfate, vitamin E, and glycosphingolipids in skin and kidney sections of patients with Fabry disease using the combined approaches of MALDI-TOF and cluster-TOF-SIMS was demonstrated by Touboul *et al.* (2007). The MALDI-based imaging technique was also used to visualize energy metabolism in the mouse hippocampus via imaging of energy-related metabolites. Cellular metabolic processes use ATP as an energy source and converting it into ADP or AMP. Thus the imaging of these molecules in tissue samples can provide useful information about energy production and how it can be used in the function of tissue (Sugiura *et al.*, 2011). The phenomenon of energy metabolism is shown in Figure 20.

Metabolomics studies of plants have also been performed to elucidate the structure, function, and biosynthetic pathways (Lisec *et al.*, 2006). Carbohydrates, amino acids, vitamins, hormones, flavonoids, phenolics, and glucosinolates are the main metabolites found in plants and are needed for growth, stress adaptation, and defense (Hounsome *et al.*, 2008). In combination with soft ionization methods such as ESI and MALDI, MS proved useful for direct analysis of plant tissue sections. The spatial distribution of sugars, metabolites, and lipids in plant tissue samples was investigated using MALDI-IMS. Cha *et al.* (2009) exploited the use of

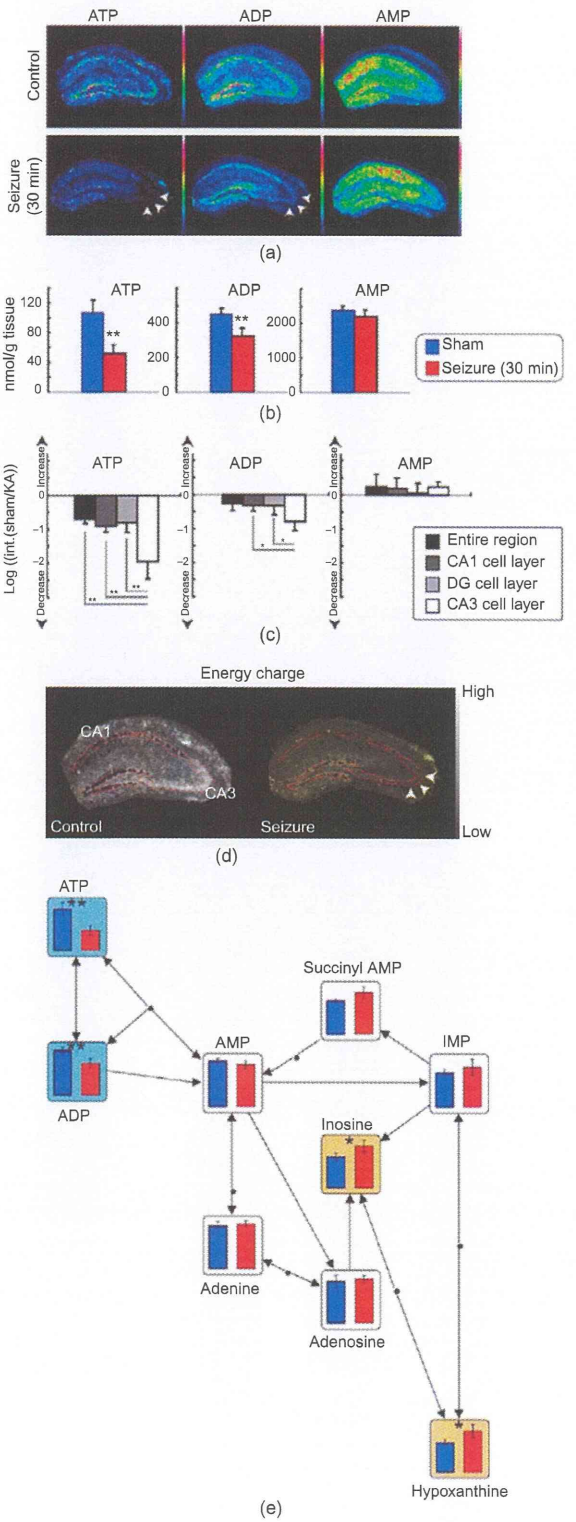

FIGURE 20 (Continued)

FIGURE 20 CA3 cell-selective consumption of adenosine triphosphate (ATP) and adenosine diphosphate (ADP) during a kainate-induced seizure. (a) MALDI imaging of adenosine nucleotides in a mouse hippocampus. (b) Absolute quantification of ATP, ADP, and adenosine monophosphate (AMP) in a mouse cerebrum using CE-MS. Massive reductions in the levels of ATP and ADP, but not AMP, were observed during kainate-induced seizures. (c) Results of the relative quantification of ion intensity for ATP, ADP, and AMP calculated from the averaged mass spectra of each hippocampal subregion obtained using MALDI imaging. The values shown are logarithmic ratios of ion intensities between sham-operated (sham) and kainate-treated mice (KA). (d) Mapping of energy-charge index values on tissue sections. The region-specific reduction of these values in the CA3 region (arrows) suggests massive energy metabolism in CA3 neurons. (e) Relative quantitative comparison of adenosine nucleotides and related metabolites using CE-MS. Each result is mapped on the metabolic pathway and clearly shows the depletion of ATP and ADP due tp their conversion into downstream metabolites. The colored graphs indicate significant increases (orange) and decreases (blue). IMP, inosine 5′-monophosphate. Reprinted from Sugiura *et al.* (2011) with permission from Public Library of Science.

colloidal silver NPs for direct profiling of an epicuticular wax on leaves and flowers from *Arabidopsis thaliana* in LDI-IMS. Recently, Goto-Inoue *et al.* (2010b) illustrated the spatial distribution of gamma-aminobutyric acid (GABA) in the seed of eggplant and the presence of GABA was confirmed by MS/MS analysis. The localization of GABA in eggplant is shown in Figure 21. Zhang *et al.* (2007) showed imaging and identification of fatty acids, sugars, and other small metabolites using colloidal graphite NPs in GALDI-IMS, which was free from matrix background noise in the low molecular region. The distribution of lysophosphatidylcholine and PC in rice endosperm and bran and alpha-tocopherol in the germ has also been reported (Zaima *et al.*, 2010).

8. SUMMARY

Several advances in sample preparation, ionization, and MS instrumentation have been achieved, steadily improving sensitivity, spatial resolution, and identification capabilities for MALDI-IMS. These improvements are broadening the MS imaging applications for lipid, peptide, and protein biomarker identification, as well as drug and metabolite imaging. Nano-PALDI, the use of ionic matrices, and the mass sicroscope techniques are new developments that could be powerful tools in obtaining high-resolution images for biomolecular distribution in biological samples. In the future, MALDI-IMS has the potential to become a routine tool for imaging of tissues, helping us to understand the link between the localization of certain molecules and their function during pathogenesis, disease progression, or treatment.

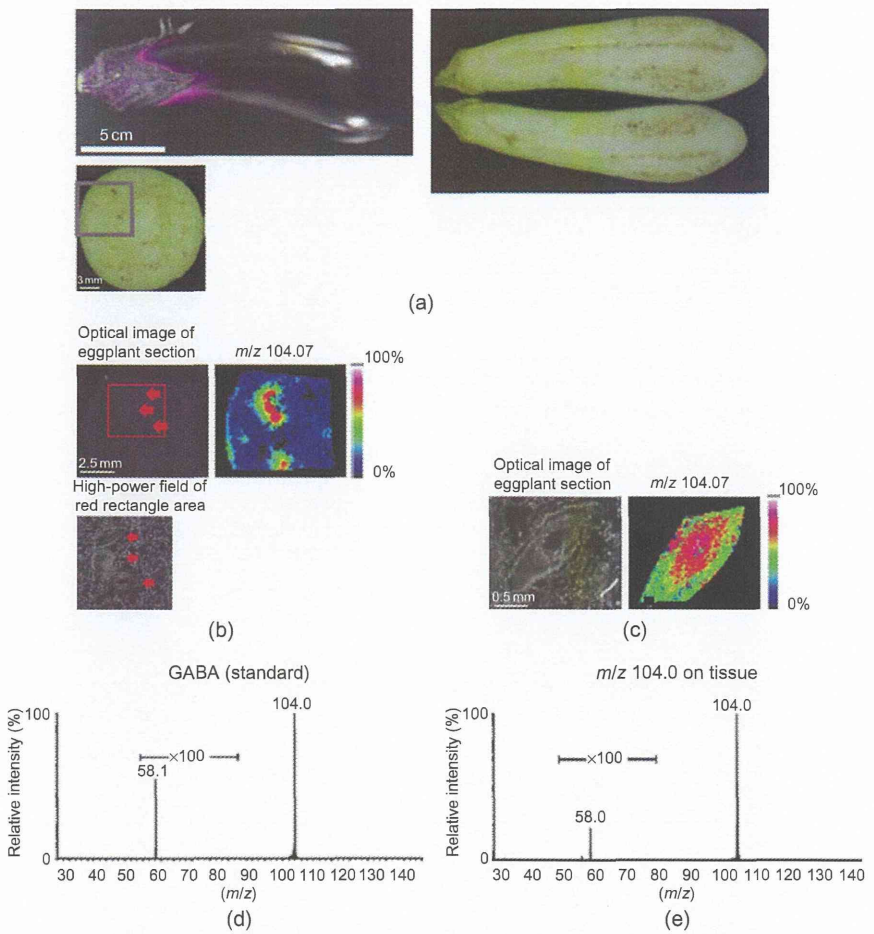

FIGURE 21 Optical images of eggplant, the results of IMS and tandem mass analyses. (a) Optical images of eggplant, vertically cut eggplant, and round-cut eggplant. A grey rectangle in a round-cut image shows the region of analyses by IMS. (b) Optical image of eggplant section and ion image of the *m/z* values at 104.07. The red arrows in the optical image show seed locations. Scale bar: 2.5 mm. Reproducibility was confirmed ($n = 3$). (c) Optical image of eggplant section and ion image of the *m/z* values at 104.07 with higher spatial resolution at 25 μm on a seed. Scale bar: 0.5 mm. (d) The tandem mass spectrum of standard gamma-aminobutyric acid (GABA) and (e) *m/z* 104.0 on eggplant tissue. Reprinted from Goto-Inoue *et al.* (2010b) with permission from The Japan Society for Analytical Chemistry.

ACKNOWLEDGMENTS

We thank the Japanese Society for the Promotion of Science, Japan, for a postdoctoral fellowship (to K.S.). This work was also supported by a grant-in-aid for SENTAN from the Japan Science and Technology

Agency (to M.S.). Cecilia Eriksson (Medical Mass Spectrometry, Uppsala University) is acknowledged for assistance in developing this chapter.

REFERENCES

Adachi, J., Kumar, C., Zhang, Y., Olsen, J. V., & Mann, M. (2006). The human urinary proteome contains more than 1500 proteins, including a large proportion of membrane proteins. *Genome Biology, 7*, R80.

Aerni, H. R., Cornett, D. S., & Caprioli, R. M. (2006). Automated acoustic matrix deposition for MALDI sample preparation. *Analytical Chemistry, 78*, 827–834.

Altelaar, A. F. M., Luxembourg, S. L., McDonnell, L. A., Piersma, S. R., & Heeren, R. M. (2007). Imaging mass spectrometry at cellular length scales. *Nature Protocol, 2*, 1185–1196.

Ametamey, S. M., Honer, M., & Schubiger, P. A. (2008). Molecular imaging with PET. *Chemical Review, 108*, 1501–1516.

Aoki, Y., Toyama, A., Shimada, T., Sugita, T., Aoki, C., Umino, Y.,... Sato, T. A. (2007). A novel method for analyzing formalin-fixed paraffin-embedded (FFPE) tissue sections by mass spectrometry imaging. *Proceedings of the Japan Academy, Series B, 83*, 205–214.

Armstrong, D. W., Li-Kang, Z., He, L., & Gross, M. L. (2001). Ionic liquids as matrixes for matrix-assisted laser desorption/ionization mass spectrometry. *Analytical Chemistry, 73*, 3679–3686.

Astigarraga, E., Barreda-Gómez, G., Lombardero, L., Fresnedo, O., Castaño, F., Giralt, M. T.,... Fernández, J. A. (2008). Profiling and imaging of lipids on brain and liver tissue by matrix-assisted laser desorption/ionization mass spectrometry using 2-mercaptobenzothiazole as a matrix. *Analytical Chemistry, 80*, 9105–9114.

Baluya, D. L., Garrett, T. J., & Yost, R. A. (2007). Automated MALDI matrix deposition method with inkjet printing for imaging mass spectrometry. *Analytical Chemistry, 79*, 6862–6867.

Benabdellah, F., Touboul, D., Brunelle, A., & Laprevote, O. (2009). In situ primary metabolites localization on a rat brain section by chemical mass spectrometry imaging. *Analytical Chemistry, 81*, 5557–5560.

Benninghoven, A. (1973). Surface investigation of solids by the statical method of secondary ion mass spectroscopy (SIMS). *Surface Science, 35*, 427–457.

Brown, H. A. (2007). *Lipidomics and Bioactive Lipids: Mass-Spectrometry–Based Lipid Analysis* (Methods in Enzymology, Vol. 432). Academic Press, Boston.

Bruker Daltonics GmbH. Bremen, Germany. Retrived from http://www.bdal.com GmbH.

Bunch, J., Clench, M. R., & Richards, D. S. (2004). Determination of pharmaceutical compounds in skin by imaging matrix-assisted laser desorption/ionization mass spectrometry. *Rapid Communications for Mass Spectrometry, 18*, 3051–3060.

Caprioli, R. M., Farmer, T. B., & Gile, J. (1997). Molecular imaging of biological samples: Localization of peptides and proteins using MALDI-TOF-MS. *Analytical Chemistry, 69*, 4751–4760.

Cazares, L. H., Troyer, D., Mendrinos, S., Lance, R. A., Nyalwidhe, J. O., Beydoun, H. A.,... Semmes, O. J. (2009). Imaging mass spectrometry of a specific fragment of mitogen-activated protein kinase/extracellular signal-regulated kinase kinase kinase 2 discriminates cancer from uninvolved prostate tissue. *Clinical Cancer Research, 15*, 5541–5551.

Cha, S., Song, Z., Nikolau, B. J., & Yeung, E. S. (2009). Direct profiling and imaging of epicuticular waxes on Arabidopsis thaliana by laser desorption/ionization mass spectrometry using silver colloid as a matrix. *Analytical Chemistry, 81*, 2991–3000.